Journal of Anatomy

J. Anat. (2014) **225**, pp60–70 doi: 10.1111/joa.12189

Comparative study of the shell development of hard- and soft-shelled turtles

Hiroshi Nagashima,[1] Masahiro Shibata,[1] Mari Taniguchi,[2,3] Shintaro Ueno,[2,3] Naoki Kamezaki[2,3] and Noboru Sato[1]

[1]*Division of Gross Anatomy and Morphogenesis, Niigata University Graduate School of Medical and Dental Sciences, Niigata, Japan*
[2]*Suma Aqualife Park, Kobe, Japan*
[3]*Sea Turtle Association of Japan, Hirakata, Japan*

Abstract

The turtle shell provides a fascinating model for the investigation of the evolutionary modifications of developmental mechanisms. Different conclusions have been put forth for its development, and it is suggested that one of the causes of the disagreement could be the differences in the species of the turtles used – the differences between hard-shelled turtles and soft-shelled turtles. To elucidate the cause of the difference, we compared the turtle shell development in the two groups of turtle. In the dorsal shell development, these two turtle groups shared the gene expression profile that is required for formation, and shared similar spatial organization of the anatomical elements during development. Thus, both turtles formed the dorsal shell through a folding of the lateral body wall, and the Wnt signaling pathway appears to have been involved in the development. The ventral portion of the shell, on the other hand, contains massive dermal bones. Although expression of HNK-1 epitope has suggested that the trunk neural crest contributed to the dermal bones in the hard-shelled turtles, it was not expressed in the initial anlage of the skeletons in either of the types of turtle. Hence, no evidence was found that would support a neural crest origin.

Key words: carapace; marker genes; neural crest; plastron; turtles.

Introduction

The turtle shell has been used as a model to understand the evolution of developmental mechanisms (reviewed by Kuratani et al. 2011). Its dorsal portion is termed the carapace, and contains ribs and vertebrae (Fig. 1, left). The skeletons are surrounded marginally with dermal bones. The rostral margin of the carapace is occupied by a nuchal plate, the lateral margin by peripheral plates, and the caudal margin by suprapygal plates and a pygal plate (Fig. 1, left). In many chelonian species, these bony structures are covered with keratinous tissue, whereas in some species, such as the soft-shelled turtles, the epidermis of the shell is not keratinized and the peripheral, suprapygal and pygal plates are often lost (Ogushi, 1911). On the other hand, the plastron is composed of nine dermal bones (Fig. 1, right). A pair of rostralmost bones, or the epiplastron, is the homologue of a clavicle. The entoplastron is more medially located, and is homologous to the interclavicle. The remaining caudal elements can be compared to gastralia (Parker, 1868; Gegenbaur, 1898; Goodrich, 1930; Zangerl, 1939, 1969; Romer, 1956; Gaffney, 1990; Claessens, 2004; also see Ogushi, 1911).

The main reason that the turtle shell has been used as one of the evo-devo models is that the turtle shell, or rib cage, encases the shoulder girdle, standing in contrast to the situation with other tetrapods, in which the girdle is outside the rib cage (reviewed by Burke, 1989, 2009; Rieppel, 2001; Gilbert et al. 2008; Kuratani et al. 2011; Nagashima et al. 2012a,b). Due to this reversed topology, the turtle carapace has been regarded as a typical example of an evolutionary novelty (reviewed by Hall, 1998; Rieppel, 2001; Gilbert et al. 2001, 2008). Because there is no intermediate pattern between the two topologies, inside or outside the ribcage, the evolution of the turtle was believed to have been saltatorial (Rieppel, 2001; Theißen, 2006, 2009; Carroll, 2012). Until the discovery of *Odontochelys* (Li et al. 2008), the oldest well-known fossil turtle, *Proganochelys,* had supported this deduction, as it already had a fully developed shell (Gaffney, 1990).

Correspondence
Hiroshi Nagashima, Division of Gross Anatomy and Morphogenesis, Niigata University Graduate School of Medical and Dental Sciences, 1-757 Asahimachi-dori, Niigata 951-8510, Japan. T: + 81 25 2272048; F: + 81 25 2270752;
E: nagahiro@med.niigata-u.ac.jp

Accepted for publication *18 March 2014*
Article published online *23 April 2014*

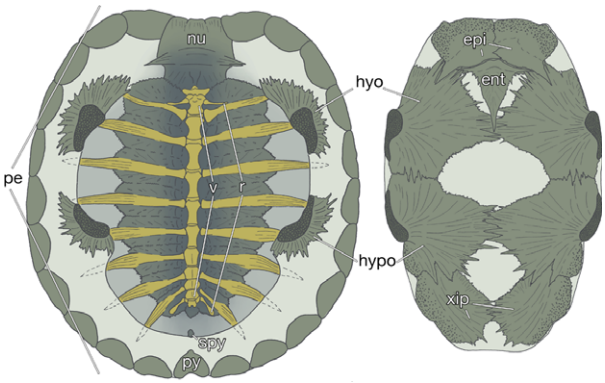

Fig. 1 The turtle shell. Inside views of the carapacial (left) and plastral (right) skeletons of a hard-shelled turtle, *Trachemys scripta elegans* (carapace length 7.3 cm). ent, entoplastron; epi, epiplastron; hyo, hyoplastron; hypo, hypoplastron; nu, nuchal plate; pe, peripheral plate; py, pygal plate; r, dorsal ribs; spy, suprapygal plate; v, dorsal vertebrae; xip, xiphiplastron.

To explain the inside-out morphology, Ruckes (1929) emphasized the importance of the repatterning of the turtle ribs during early development, and hypothesized that the turtle makes a specialized dermis – the carapacial dermis – that captures the rib anlagen and brings them dorsally and laterally over the scapular anlage, resulting in the topological change between the skeletal elements. Burke (1989, 1991) proposed that the redirection of the rib growth trajectory was caused by the carapacial ridge (CR) (Fig. 2; reviewed by Burke, 2009). The CR appears on the lateral aspect of the flank of turtle embryos and forms the leading edge of the developing carapace. Histologically, it consists of an aggregated mesenchyme with overlying thickened epidermis, a configuration which resembles the distal tip of the tetrapod limb bud (Burke, 1989). The distal limb bud is known as the site of epithelial–mesenchymal interaction. The reciprocal inductive interaction between fibroblast growth factor (FGF) 8 emanated from an epidermis (apical ectodermal ridge; AER) and FGF10 from the underlying mesenchyme is essential for the limb outgrowth and proximodistal patterning of the limb skeleton (reviewed by Tabin & Wolpert, 2007, and references therein).

Following these studies, the paracrine hypothesis proposed that a reciprocal interaction between the CR and ribs played a pivotal role in the topological shift (Cebra-Thomas et al. 2005). As in the limb bud, *Fgf10* expression was reported in the CR mesenchyme (Loredo et al. 2001), and *Fgf8* in the distal tip of ribs in the hard-shelled turtle *Trachemys scripta* (Cebra-Thomas et al. 2005). The hypothesis explains that in other amniotes the rib precursor cells migrated ventrally between the muscle plates, the elongated myotome, into the lateral body wall, whereas in turtles, FGF10 from the CR attracted rib precursor cells laterally and dorsally, and the ribs moved through the muscle plate to enter the CR. A positive feedback loop between the FGFs secreted from the CR and the ribs, similar to that of the limbs, maintained the CR and caused the co-ordinated growth of the carapacial plate and the ribs. In support of the theory, it was reported that FGF inhibitor caused the degeneration of the CR with the extension of the ribs into the lateral body wall, whereas chicken ribs were attracted to FGF10-soaked beads (Cebra-Thomas et al. 2005). This hypothesis is based on co-option (review by True & Carroll, 2002) – the recruitment of limb developmental programs into the turtle flank (Loredo et al. 2001) – and can explain the rapid evolution of turtles (reviewed by Gilbert et al. 2008; also see Pennisi, 2004; Nagashima et al. 2012a,b).

However, a study used the soft-shelled turtle *Pelodiscus sinensis* reported that the CR did not express the *Fgfs*, and that it expressed genes related to the Wnt signaling pathway: *cellular retinoic acid-binding protein (Crabp)-I, Sp-5, lymphocyte enhancer factor (Lef)-1* and *Apcdd-1* (Kuraku et al. 2005). In addition to these, expression of *hepatocyte growth factor* (*HGF*) was found in the vicinity of the CR (Kawashima-Ohya et al. 2011). Inhibition of these signaling cascades abolished the CR, implying the involvement of the genes to the development of the CR (Nagashima et al. 2007; Kawashima-Ohya et al. 2011). Contrary to those previous views, Nagashima et al. (2007) contended that the CR could not attract migrating rib precursor cells, and instead functioned in the turtle specific rostro-caudal expansion of rib arrangement through its active growth (also see Burke, 1989). For the topological change between the skeletons, the folding theory (Nagashima et al. 2009) argued that the trajectory of turtle ribs was the same as that in other amniotes, since ribs grow along the muscle plate even in turtles. However, the turtle ribs are arrested in the axial domain, expand laterally and rostrocaudally, and cover the shoulder girdle caudodorsally by folding the lateral body wall inward, resulting in encapsulation of the shoulder girdle under the ribs. The folding occurred late in development, not early as the former views assumed, and did not change the topological relationships between the ribs, muscle plate and shoulder girdle from those at the beginning of the development. According to this theory, since the topology between the anatomical elements is conserved between turtles and other amniotes, it is possible to infer the gradual evolution of turtles (Nagashima et al. 2009; reviewed by Kuratani et al. 2011; Nagashima et al. 2012a,b).

For the different expression patterns of *Fgfs*, the species differences in turtles have been suggested (Cebra-Thomas et al. 2005; Gilbert et al. 2008; also see Lubick, 2013): the paracrine hypothesis was based on the observation of the hard-shelled turtle *T. scripta*, while the folding theory the soft-shelled turtle *P. sinensis*. This proposal suggests a possibility that these two groups of turtles utilized distinct mechanisms to form the carapace, because *Fgfs* occupy a vital position in the paracrine hypothesis. Actually, in the hard-shelled turtles, the topologies between ribs, muscle

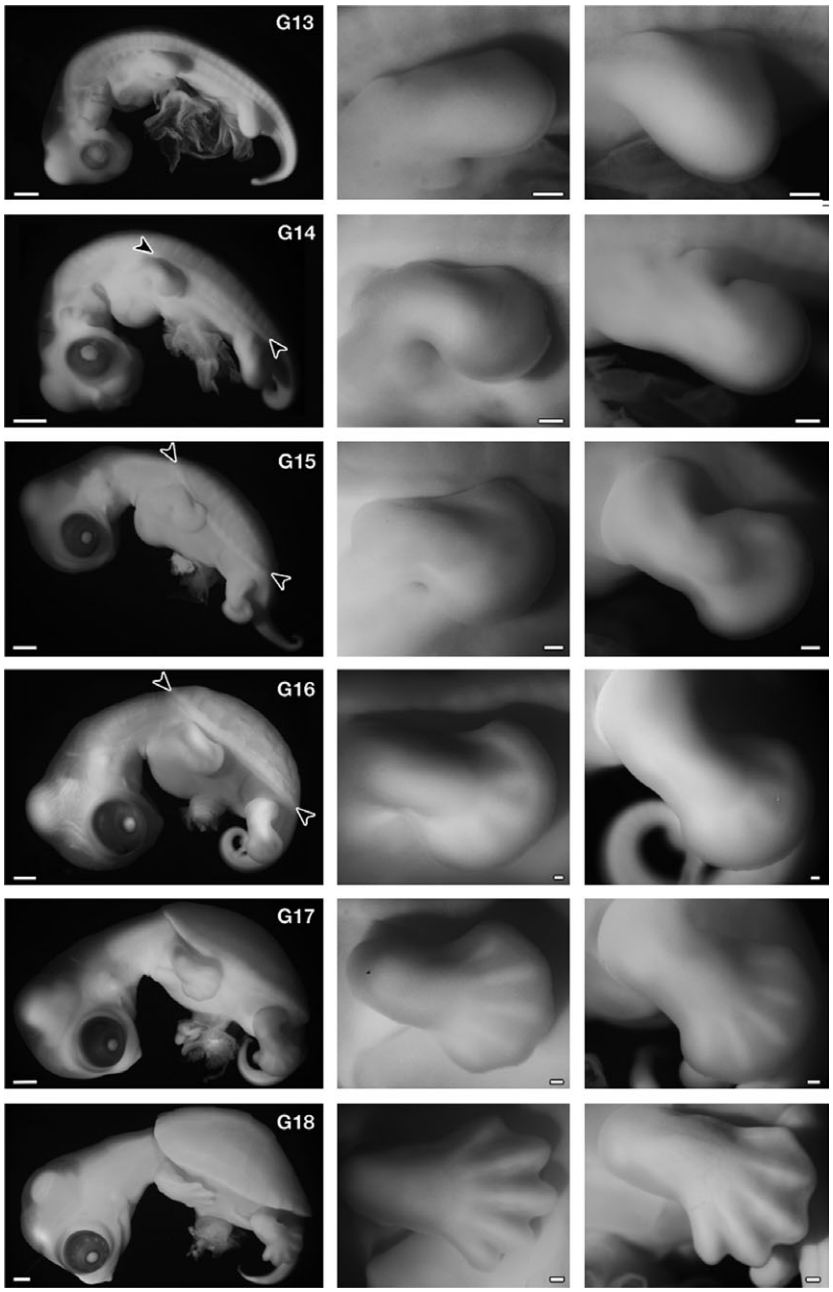

Fig. 2 Development of *Trachemys scripta*. (Left) Left lateral view of the embryos. (Middle) Forelimb. (Right) Hindlimb. In G stage 14, carapacial ridge (CR) appears as a longitudinal ridge in the flank (arrowheads), and in stage 15, the CR acquires a segmental pattern (arrowheads). The ridge comprises the margin of the carapace in the latter stages. The morphology of the forelimb bud is comparable to that in *Chelydra serpentina* (Yntema, 1968) and *Pelodiscus sinensis* (Tokita & Kuratani, 2001) at the same stage. Namely, in G stage 13, the length is longer than the width, and G stage 14 is an early paddle stage with a digital plate, in G stage 15 the digital plate is well formed without a digital groove, in G stage 16 digital ridges appear, in G stage 17 the periphery of the digital plate shows a slight serration and five digits are apparent, and in G stage 18 the periphery of the digital plate is serrated deeply, similar to that of maple leaves. Scale bars: 1 mm (left column), 200 μm (middle and right columns).

plate, and shoulder girdle are presumed to have been altered from those in other amniotes in early development (Cebra-Thomas et al. 2005), whereas in the soft-shelled turtles, they are reported to have been basically conserved (Nagashima et al. 2009).

In the present study, to confirm the above possibility, we observed the *Fgfs* expressions and the anatomical organizations in *T. scripta elegans,* and compared them with those in *P. sinensis*. During development of the CR and rib anlagen in *T. scripta*, the *Fgfs* were not expressed in these tissues, whereas *Wnt5a* and its related genes were expressed either in or near the developing CR. In *T. scripta,* the ribs developed along, rather than through, the muscle plate, which was folded ventromedially inside the shoulder girdle; a similar topological pattern to that in *P. sinensis*. Thus, the developmental mechanisms of the dorsal shell were conserved between the two turtle groups.

The second argument has to do with the ontogenetic origin of dermal bones in the turtle shell. In chickens and mice, the major dermal skeleton is the calvarium (dermal skull roof), most of which is made up of a cephalic neural crest (reviewed by Gross & Hanken, 2008); thus, it tends to be accepted that the dermal bones were derived from neural crest cells (Moss, 1969; Smith & Hall, 1990; also see Hall, 1998; Vickaryous & Sire, 2009). Some of the dermal bones in

the turtle flank, the nuchal plate and plastral bones, are suggested to be derivatives of the trunk neural crest (Clark et al. 2001; Cebra-Thomas et al. 2007, 2013; Gilbert et al. 2007; reviewed by Gilbert et al. 2008; also see Pennisi, 2004). According to this proposal, these trunk neural crest cells are unique to turtles in that they appear dorsal to the neural tube in the late developmental period and possess skeletogenic potency. Because the trunk crest cells in other amniote model animals cannot form skeletons under normal conditions (Le Douarin et al. 1977; Nakamura & Ayer-le Lievre, 1982; also see McGonnell & Graham, 2002; Abzhanov et al. 2003; reviewed by Gross & Hanken, 2008), it is hypothesized that the turtle crest cells acquire the competence by losing the *Hox* expression of the trunk – a co-option of skeletogenic competence from the cephalic neural crest to the trunk neural crest (Cebra-Thomas et al. 2007, 2013; Gilbert et al. 2008). This proposition is supported by expressions of marker genes and proteins, cell lineage analysis using lipophilic dye, and *in vitro* culture of neural tube explant of *T. scripta* (reviewed by Gilbert et al. 2008). In particular, the expression of the HNK-1 epitope, which is often used to recognize early migrating neural crest cells in chickens, has been adopted as the most important evidence.

This theory has, however, been confronted with data showing that early anlagen of the plastral bones in *P. sinensis* show no immunoreactivity for the antibody (Kuratani et al. 2011). For this discrepancy, differences in the fixatives used have been suggested (Kuratani et al. 2011). And again, this could be ascribed to the species differences.

In this study, we observed the expression of HNK-1 epitope in the two turtle species and in chickens as an outgroup species, and found that although the developing plastral bones in *T. scripta* showed immunoreactivity, their initial anlagen did not express the epitope as those in *P. sinensis*. Considering the expression pattern in these animals, the expression of the epitope in *T. scripta* plastral bones appears to be a species-specific trait associated with ossification, not with particular cell lineage.

Materials and methods

Sample collection

Fertilized eggs of *Trachemys scripta elegans* (red-eared slider) were collected in the Suma aquarium in Kobe and were incubated at 27 °C. The embryos were staged according to a table established by Greenbaum (2002). Fertilized eggs of *Pelodiscus sinensis* were purchased from a local farm in Japan. The eggs were incubated at 30 °C, and the embryos were staged according to a table established by Tokita & Kuratani (2001). Fertilized chicken eggs were also obtained from a local supplier and incubated at 38 °C. The embryos were staged according to a method established by Hamburger & Hamilton (1951). Animal care was entirely in accordance with the guidelines provided by Niigata University, and approval for the experiments was obtained from the institutions.

Histology, immunohistochemistry and 3D reconstruction

Embryos were fixed with Serra's fixative (Serra, 1946). Hematoxylin and eosin (HE) followed by 0.1% Alcian blue were used to stain 8-μm-thick paraffin sections. Immunohistochemistry was performed using anti-CD57 (HNK-1, BD Pharminogen, San Diego, CA, USA; 1 : 40). A Vectastain ABC Elite kit (Vector Laboratories, Burlingame, CA, USA) was used to visualize the immunoreaction. All images were recorded with a DP70 digital camera (Olympus Corporation, Shinjuku, Tokyo, Japan) attached to a light microscope. Histological sections stained with HE-Alcian blue were reconstructed with AVIZO® (Visualization Sciences Group, Burlington, MA, USA).

cDNA cloning and in situ hybridization

Trachemys scripta elegans APCDD1, Fgf8, Fgf10, HGF, and *Wnt5a* homologue genes were obtained by degenerate RT-PCR. We designed primers based on the nucleotide sequence of putative orthologue sequences found in the genome obtained by the painted turtle *Chrysemys picta bellii* genome project (http://genome.wustl.edu/genomes/detail/chrysemys-picta-bellii/). The identified sequences have been deposited in GenBank under accession numbers **AB896700–4**. The *in situ* hybridization was performed as described previously (Nagashima et al. 2007).

Results

Comparison of the developmental stages between *T. scripta* and *P. sinensis*

First, we confirmed that the two developmental tables for *T. scripta* (Greenbaum, 2002) (G stages) and *P. sinensis* (Tokita & Kuratani, 2001) (TK stages) were comparable during stages 13–18 based on external morphology and histological characteristics in the shoulder region (compare Fig. 2 and Tokita & Kuratani, 2001; also see below). Although Greenbaum (2002) reported that the CR appears in the G stage 15 as an 'irregular longitudinal ridge', the ridge could be observed in G 14 as a continuous longitudinal swelling (Fig. 2, arrowheads).

Gene expressions and morphological change involved in carapace formation

The expressions of *Fgfs* mRNAs were examined in *T. scripta* embryos. As with chickens (Crossley et al. 1996; Sánchez-Guardado et al. 2013), *Fgf10* and *8* were expressed in the otic vesicle and in the AER of the hindlimb bud in G stage 13 embryos, respectively (Fig. 3A,B). *Fgf10* expression was not observed in the limb mesenchyme (Supporting Information Fig. S1A). These expression patterns in the limb bud are consistent with those in chickens. This is because the morphology of the limb in G 13 *T. scripta* embryos is the same as that in TK stage 13 *P. sinensis* (compare Fig. 2 and Tokita & Kuratani, 2001), which is equivalent to Hamburger & Hamilton stage (1951; HH stage) 24 chickens (Nagashima

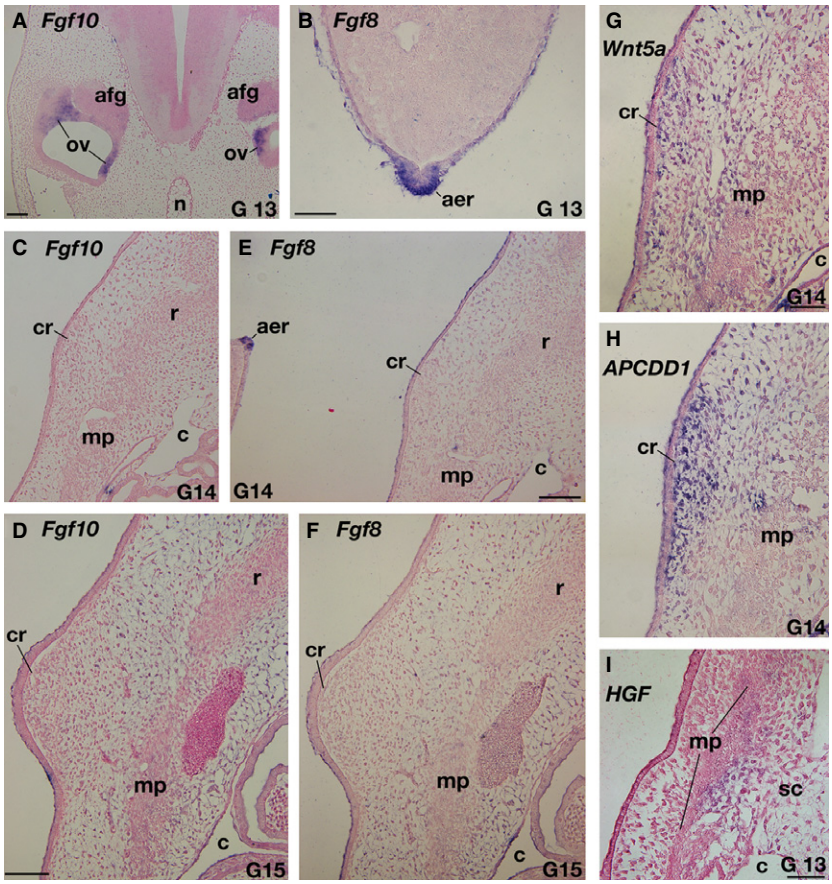

Fig. 3 Expressions of genes related to the carapace development in *Trachemys scripta*. (A–F) Expressions of *Fgfs*. (A,B) Positive controls. In G stage 13 embryo, *Fgf10* (A) and *Fgf8* (B) are expressed in the otic vesicle (ov) and apical ectodermal ridge (aer) in the hindlimb bud, respectively. (C–F) *Fgf10* (C,D) and *Fgf8* (E, F) expressions in the carapacial ridge (cr) and its adjacent area. (E, F) Adjacent sections to (C,D), respectively. Note that both in G stage 14 (C,E) and 15 (D,F), these genes are not expressed in the CR and ribs, whereas AER is positive for the *Fgf8* probe (E). (G–I) Expressions of Wnt-related genes. (H) Adjacent section to (G). *Wnt5a* (G) and *APCDD1*(H) are expressed in the mesenchyme of the CR, whereas *HGF* (I) is expressed in the lateral sclerotome (sc). afg, acoustico-facialis ganglion; c, coelom; mp, muscle plate; n, notochord. Scale bars: 100 μm (A,C–F), 50 μm (B, G–I).

et al. 2005), and chicken *Fgf10* expression is already decreased at this stage before the downregulation of *Fgf8* (Ohuchi et al. 1997). These expressions confirm that the experimental procedures were appropriate. These genes were, however, expressed neither in the CR or in the rib primordia from G stage 13–15 embryos (Figs 3C–F, S1B-S1E; data not shown for G stage 13). On the other hand, genes expressed in the CR and its vicinity in *P. sinensis* (Kuraku et al. 2005; Kawashima-Ohya et al. 2011; Wang et al. 2013) were expressed in the *Trachemys* embryos. Namely, *Wnt5a* was expressed in the CR mesenchyme and one of the target genes of the Wnt signaling pathway, *APCDD1* (Takahashi et al. 2002; Shimomura et al. 2010) showed strong expression in the CR mesenchyme, whereas *HGF* was weakly expressed in the lateral sclerotome (Fig. 3G–I). These expression patterns in *T. scripta* were almost identical to those in *P. sinensis*, although *APCDD1* was negative in the CR epidermis.

The similarities of the gene expression patterns imply that the two turtle species share the same developmental mechanisms in the carapace formation. To confirm the topological relationships between the anatomical elements in *Trachemys*, histological sections were reconstructed at the brachial-thoracic level. In G stage 17 embryos, ribs had already extended laterally and were restricted to the dorsal axial domain (Fig. 4; Supporting Information Movie S1). They were, however, observed along the muscle plate, which was folded ventromedially. The shoulder girdle was situated outside the muscle plate. This morphological pattern is completely the same as that in *P. sinensis* embryos (Nagashima et al. 2009). Thus, the carapace formation of *T. scripta* also occurred via a folding of the lateral body wall.

HNK-1 reactivity of turtle embryos

Trachemys scripta embryos were fixed with Serra's fixative because it was suggested that 4% paraformaldehyde in phosphate-buffered saline could produce non-specific signals, whereas the former fixative contained acetic acid, stabilizing the HNK-1 epitope (Kuratani et al. 2011).

In *T. scripta* embryos, the signals were observed in the spinal nerve, dorsal root ganglia, sympathetic ganglia and spinal cord (Fig. 5A–C), which are known to be positive for the antibody in chickens and *P. sinensis* (Bronner-Fraser, 1986; Kuratani et al. 2011), guaranteeing the procedures for immunostaining. The reactivity was found in the mesenchyme dorsal to the neural tube in G stages 17–18 (Fig. 5A–F). The signal was narrow in G stage 17 (Fig. 5E) but had expanded in the later stage (Fig. 5F). The staining

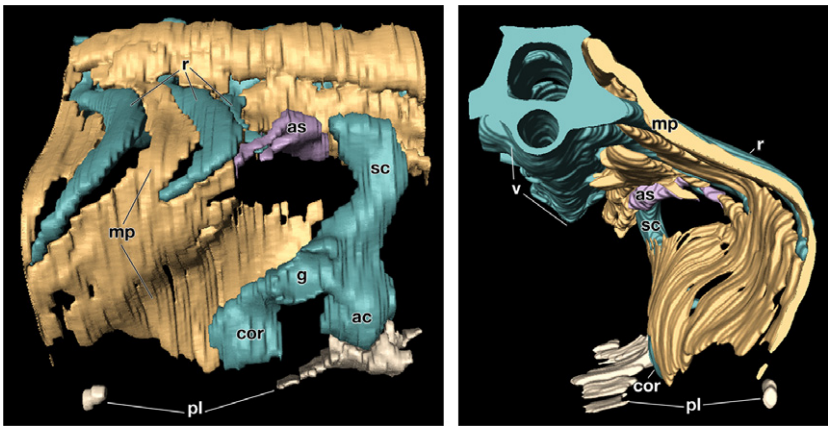

Fig. 4 Three-dimensional reconstruction of the shoulder region of G stage 17 *Trachemys scripta* embryo. (Left) Lateral view. Rostral is on the right. Note that the shoulder girdle is rostro-lateral to the muscle plate. (Right) Caudal view. Medial is on the left. The left half of the embryo is eliminated. Note that ribs grow along the muscle plate, which is folded medially around the shoulder girdle. ac, acromion; as, serratus anterior; cor, coracoid; g, glenoid cavity; pl, plastron; sc, scapular blade.

was also observed in the mesenchyme near the ribs (Fig. 5G, H) and the periphery of the ribs (Fig. 5I,J). The plastral bones were also positive for the antibody (Fig. 5K,L). These results were consistent with those in the previous reports (Clark et al. 2001; Cebra-Thomas et al. 2007, 2013; Gilbert et al. 2007). However, in G stage 17, the antibody did not recognize the cell aggregation that will form the plastral bones (Fig. 6A,B). This suggested that immunoreactivity in the plastral bones is acquired secondarily during osteogenesis and does not represent a particular cell lineage. To verify the assumption, the humerus was observed, because the skeleton is derived solely from the lateral plate mesoderm in chickens (reviewed by Tamura et al. 2001; Tanaka, 2013). In the rim of the humerus, the signal was observed, which was completely overlapped by the distribution of the intramembranous bone (Fig. 6C,D). Supporting the findings, the

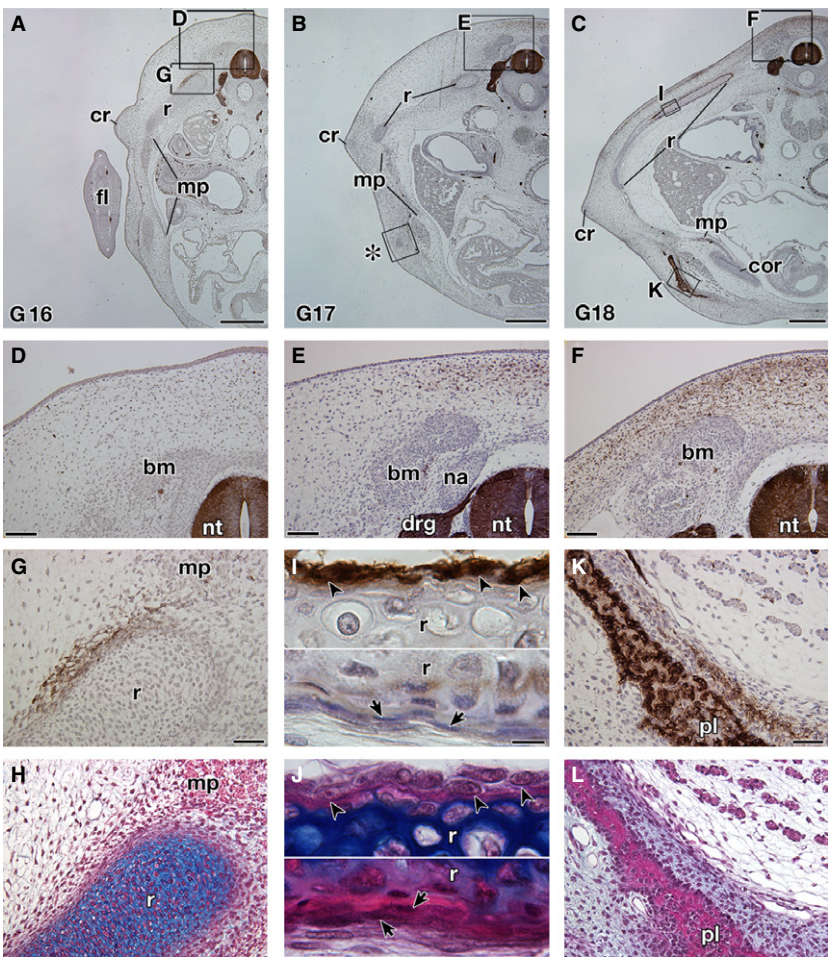

Fig. 5 Expression of the HNK-1 epitope in *Trachemys scripta* embryos. Transverse sections of *T. scripta* embryos are either stained with HNK-1 and counterstained with hematoxylin (A–G,I,K) or simply stained with hematoxylin and eosin (HE) and then Alcian blue (H,J,L). (A–C) Transverse sections at low magnification. (D–L) Higher magnification of the boxes in (A–C). (H,J, L) Adjacent sections to (G,I,K), respectively. (D–F) The dorsal part of the embryo showing the distribution of the HNK-1 epitope. Note that the HNK-1 epitope appears from G stage 17 (E) and the expression domain expands in G stage 18 (F). (G–J) Distribution of the HNK-1 epitope in the ribs. A part of the mesenchyme surrounding the ribs is HNK-1-positive (G,H). In G stage 18 (I,J), the epitope was observed in the cells with a round nucleus in the periosteum (arrowheads), whereas the cells with a long nucleus are HNK-1-negative (arrows). (K,L) Distribution of the HNK-1 epitope in the plastron of the G stage 18 embryo. Immunoreactivity was observed for the osteoblast in the plastral bones and in the adjacent mesenchyme. drg, dorsal root ganglion; fl, fore limb; na, neural arch; nt, neural tube. Scale bars: 500 μm (A–C), 100 μm (D–F), 50 μm (G,H,K,L), 20 μm (I,J).

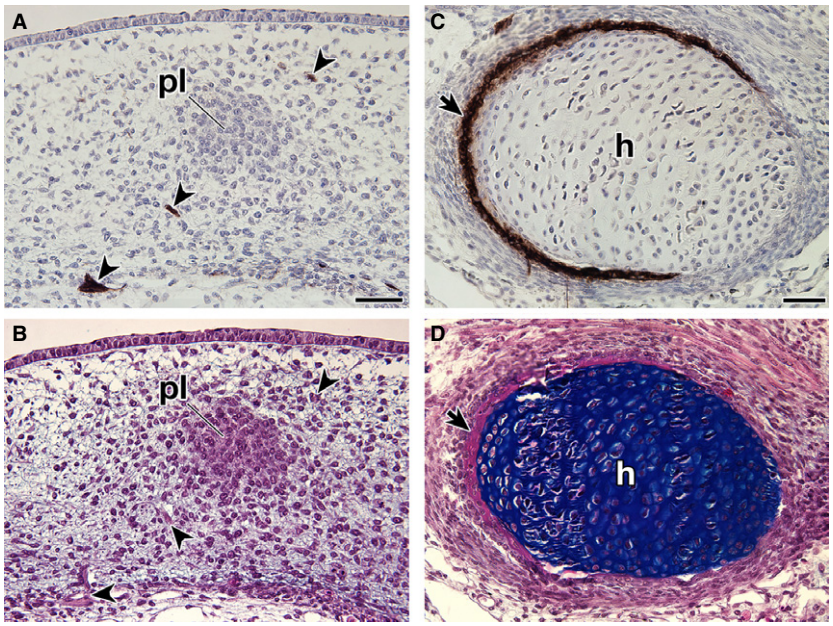

Fig. 6 Expression of the HNK-1 epitope in *Trachemys scripta* embryos. Transverse sections of *T. scripta* embryos were either stained with HNK-1 and counterstained with hematoxylin (A,C) or simply stained with HE and then Alcian blue (B,D). (B,D) are adjacent sections to (A,C), respectively. (A, B) Higher magnification of the box (asterisk) in Fig. 5B, showing distribution of the HNK-1 epitope in the initial anlage of the plastral bones in the G stage 17 embryo. Note that the anlage is HNK-1-negative, whereas the peripheral nerves are strongly stained with the antibody (arrowheads). (C,D) Distribution of the HNK-1 epitope in the humerus (h) of the G stage 18 embryo. Note that the expression domain of HNK-1 overlaps the area of the intramembranous bone (arrows). Scale bars: 50 μm.

staining in the ribs was also restricted to the intramembranous bone, particularly to cells with a round nucleus in the periosteum (Fig. 5I,J, arrowheads), whereas it was not found in cells with a long nucleus (Fig. 5I,J, arrows). From their position and morphology, the former cells appeared to represent active osteoblasts, whereas the latter more closely resembled inactive osteoblasts.

To investigate species differences of HNK-1 immunoreactivity, *P. sinensis* embryos at several stages were stained. In TK stage 11, HNK-1 antibody recognized the cell population located in the dorso-lateral part of the neural tube (Fig. 7A,B). This pattern coincided with the distribution pattern of neural crest cells in the chicken (Bronner-Fraser, 1986), confirming that the antibody can react with crest cells in the soft-shelled turtle. The plastron anlage in *P. sinensis* appeared as a cell aggregation in TK stage 17 (Fig. 7 in Kuratani et al. 2011), and deposited bone matrix in TK stage 18 (Fig. 7E). These developmental characteristics are similar to those in G stage 17 and 18 in *T. scripta*, respectively (Figs 6B and 5L). However, the mesenchyme dorsal to the neural tube was not stained by HNK-1 in *P. sinensis* –in either TK stage 17 or 18 (Fig. 7C; also see Fig. 7 in Kuratani et al. 2011). Instead, some peripheral nerves, spinal cord and intrinsic back muscles were found to be positive for the antibody (Fig. 7C). Anlagen of the plastral bones were also negative for the antibody in these stages (Fig. 7D,E; Fig. 7 in Kuratani et al. 2011). The intramembranous bones of the ribs and humerus showed no immunoreactivity in the soft-shelled turtle (Fig. 7F–I). As an out-group comparison, the intramembranous bones and dorsal mesenchyme of the neural tube showed no reactivity in HH 32, 34, and 37 chicken embryos, although some chondrocytes were positive for the antibody (Fig. 7J,K, Supporting Information Fig. S2, and data not shown).

These results indicate that the plastral bones develop from HNK-1 negative primordia in both turtle species, and that *T. scripta* have unique expression patterns for the NHK-1 epitope among amniotes in that the antibody recognizes osteoblasts as well as the dorsal mesenchyme in the particular developmental time window.

Discussion

For the turtle shell formation, different hypotheses have been proposed based on differing results between the hard-shelled turtles and the soft-shelled turtles (see above). To investigate the cause of these discrepancies, we compared their development. For the carapace formation, the basis of the paracrine hypothesis was the expressions of *Fgfs* in *T. scripta* (Loredo et al. 2001; Cebra-Thomas et al. 2005). In these experiments, *Fgf10* antisense riboprobe derived from the spiny soft-shelled turtle *Trionyx spiniferous* was applied to *T. scripta* (Loredo et al. 2001) and the expression of *Fgf8* was examined with whole-mount *in situ* hybridization (Cebra-Thomas et al. 2005). However, there remains the possibility that the *Fgf10* signal did not represent the exact expression due to species differences of the riboprobe, and the whole-mount *in situ* hybridization cannot identify the exact expression domain on a single-cell level.

To overcome these disadvantages, we prepared the riboprobes from *T. scripta,* and adopted the section *in situ* hybridization. We were unable to detect the expression of these *Fgfs* in the CR or the ribs of *T. scripta* (Figs 3C–F, S1B-S1E). These results are consistent with those in *P. sinensis* (Kuraku et al. 2005). Although Loredo et al. (2001) reported the *Fgf10* expressions both in the CR and in the limbs at the same developmental stage (23-day embryo), because *Fgf10*

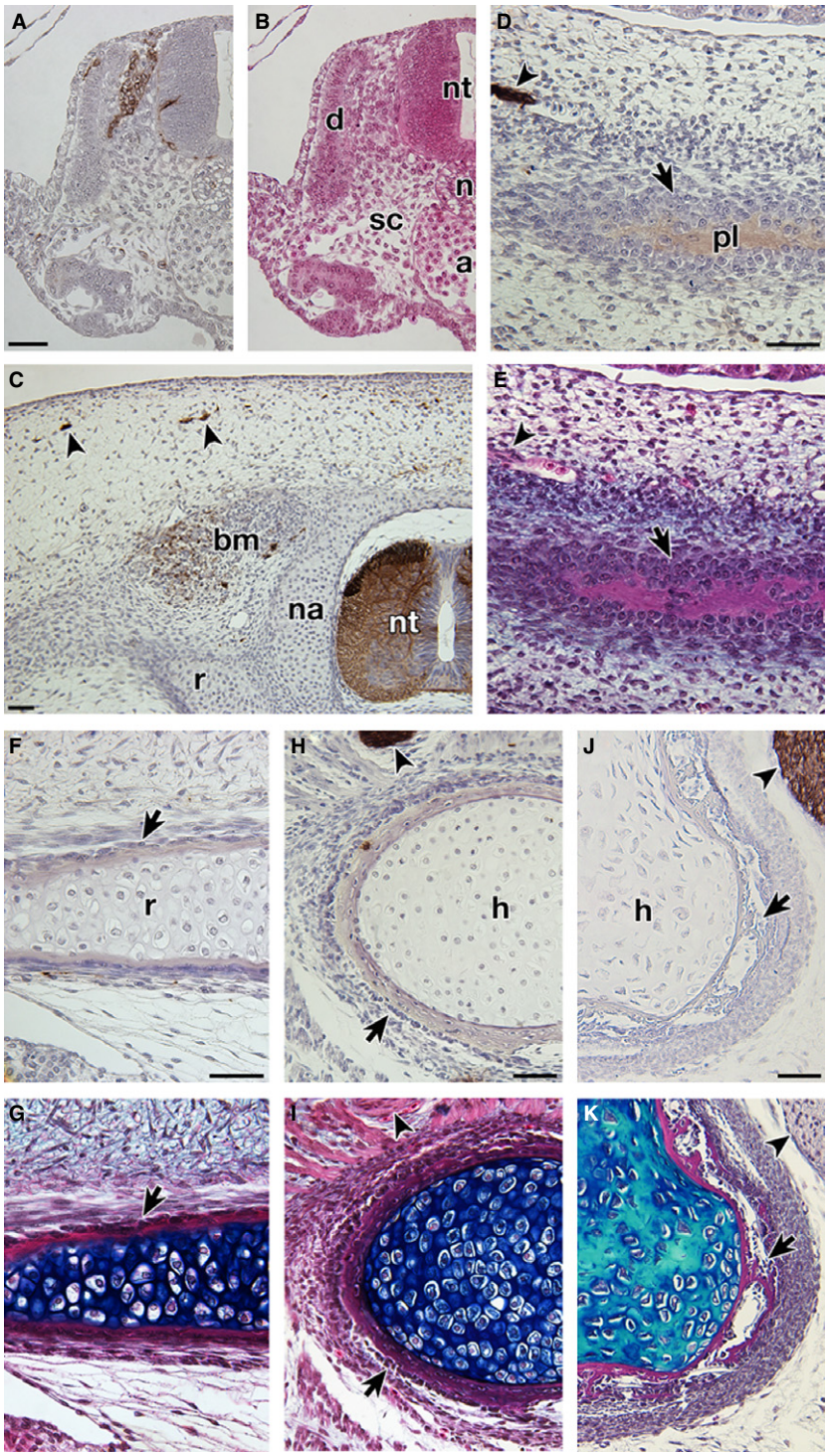

Fig. 7 Expression of the HNK-1 epitope in *Pelodiscus sinensis* and *Gallus gallus* embryos. Transverse sections of *P. sinensis* (A–I) and *G. gallus* (J,K) embryos were either stained with HNK-1 and counterstained with hematoxylin (A,C,D,F,H,J) or simply stained with HE (B) and then Alcian blue (E,G,I,K). (B,E,G,I, K) Adjacent sections to (A,D,F,H,J), respectively. (A–I) Transverse sections of *P. sinensis*. (A,B) TK stage 11 embryo. Cell population dorso-lateral to the neural tube is stained with the antibody. From its position, these cells appear to be neural crest cells. (C) The dorsal part of the TK stage 18 embryo, showing distribution of the HNK-1 epitope. Note that the dorsal mesenchyme is negative for the antibody, which recognizes only the spinal cord (nt), peripheral nerves (arrowheads) and intrinsic back muscles (bm). (D–I) Distribution of the HNK-1 epitope in the intramembranous bones. (D,E) and (F–I) are TK stage 18 and 20, respectively. Note that the intramembranous bones (arrows) in the plastral bone (D,E), ribs (F,G) and humerus (H,I) of *P. sinensis* are negative for the antibody. (J and K) Distribution of the HNK-1 epitope in the humerus of HH 37 *G. gallus* embryo. The intramembranous bone (arrows) is negative for the antibody. Arrowheads show peripheral nerves for the positive control. a, dorsal aorta; d, dermomyotome; sc, sclerotome. Scale bars: 50 μm.

expression in the limb bud has already been abolished at G 13 (Fig. S1A) before the CR development at G14 (Fig. 2) in *T. scripta*, the observation appears to be due to the background staining.

Despite the non-expression of *Fgfs*, we observed the expressions of Wnt signaling-related genes in *T. scripta* (Fig. 3G–I), as with those seen in *P. sinensis* (Kuraku et al. 2005; Kawashima-Ohya et al. 2011; Wang et al. 2013). Because the CR plays a role in carapace formation (Burke, 1989, 1991; Nagashima et al. 2007; reviewed by Kuratani et al. 2011), this finding suggests that the developmental mechanism of the carapace is shared between the two turtle groups. Actually, a 3D reconstruction of the histological sections showed that the musculoskeletal pattern in

T. scripta is similar to that found in *P. sinensis* and other amniotes (Fig. 4; Movie S1; Nagashima et al. 2009). Thus, what is unique to turtles is the axial arrest of ribs and the marginal growth of the flank caused by the CR (Burke, 1989; Nagashima et al. 2007), and these enable turtles to encase the shoulder girdle under the ribs by folding the lateral body wall inward to form the carapace (reviewed by Kuratani et al. 2011; Nagashima et al. 2012a,b).

The neural crest hypothesis for trunk dermal bones in turtles is based mainly on the immunoreactivity to HNK-1 (Clark et al. 2001; Cebra-Thomas et al. 2007, 2013; Gilbert et al. 2007; reviewed by Gilbert et al. 2008). HNK-1 antibody was prepared to recognize the epitope on human natural killer cells (Abo & Balch, 1981), which originated from the mesoderm (reviewed by Moignard et al. 2013; Yu et al. 2013). Thus, the expression of the epitope does not always show the neural crest derivatives, and *vice versa* (Luider et al. 1992, 1993). Strictly speaking, HNK-1 is only applicable to early migrating crest cells in chicken embryos, in which the distribution of crest cells has already been confirmed by cell lineage analyses, such as with chick-quail chimera (Le Douarin, 1982). This is true for other so-called marker gene and protein expressions, and a combination of these also does not support derivation of cells. Hence, the usage of HNK-1 for turtle embryos would be justified only when the immunostaining in turtle embryos is similar to the distribution of early crest cells in the chicken (Fig. 7A; Bronner-Fraser, 1986). However, the antibody can tell us nothing about cell lineage either in the older embryos or in turtle-specific structures.

Our experiments showed that the fixative was not the cause of the different results between the two turtle species for the HNK-1 immunoreactivity (see Kuratani et al. 2011), but rather many of the signals in *Trachemys* appear to have been species-specific traits associated with ossification (Figs 5I–L and 6C,D). As for other examples of staining, such as those in the dorsal mesenchyme (Fig. 5E,F), immature rib (Fig. 5G,H), back muscles (Fig. 7C) and cartilage (Fig. S2), the epitope would reflect some physiological characteristics of the cell population, but these remain unexplained (also see Nagase et al. 2000; Domowicz et al. 2003).

To analyze the developmental origin of the dermal bones, long-term cell labeling is required. Cebra-Thomas et al. (2007, 2013) have challenged the experiment by using DiI. Unfortunately, because the lipophilic dye can easily contaminate the neighboring cells, it has been mistakenly concluded from the DiI experiments that the fin mesenchymal cells also originate from the neural crest (see Lee et al. 2013a, and references therein). The application of another method, such as the introduction of green fluorescent protein, must be awaited (also see Nagashima et al. 2012b).

The neural crest hypothesis is a very intriguing because the majority of the dermal bone in the head is derived from the cephalic neural crest. The dermal skull roof, however, also has a mesodermal contribution (reviewed by Gross & Hanken, 2008). Moreover, the clavicle, which is the only dermal bone in the trunk region of mice, derives from the cephalic neural crest and the trunk mesoderm (Matsuoka et al. 2005). Recently, the dermal scales and fin ray of the medaka (teleost trunk dermal bones) were shown to derive from the trunk mesoderm (Shimada et al. 2013; also see Lee et al. 2013b; Mongera & Nüsslein-Volhard, 2013). Thus, the dermal bones do not always originate from the neural crest. For the plastral bones, a part of the rostral pair, the epiplastron, could be derived from the cephalic neural crest because these are homologous to the clavicle (Gegenbaur, 1898; Goodrich, 1930; Romer, 1956), but other dermal bones potentially could derive from the mesoderm as well as from the neural crest (reviewed by Kuratani et al. 2011; Kuratani & Nagashima, 2012). Although the origin of the plastron remains enigmatic, our study concluded that HNK-1 immunoreactivity does not provide informative evidence concerning the cell lineage of the plastral bones.

In conclusion, we found that the two turtle species utilized almost the same developmental mechanisms in the formation of their shells. Future studies will unveil the developmental origin of the plastral bones and the molecular mechanisms necessary to cause the axial arrest of the ribs.

Acknowledgement

This work was supported by grants-in-aid to H.N. from the Ministry of Education, Science and Culture of Japan.

Author contributions

H.N. and N.S. designed the research. H.N. and M.S. performed the experiments. M.T., S.U. and N.K. collected *Trachemys* eggs. H.N. and N.S. wrote the manuscript.

Conflicts of interest

The authors declare no conflicts of interest.

References

Abo T, Balch CM (1981) A differentiation antigen of human NK and K cells identified by a monoclonal antibody (HNK-1). *J Immunol* **127**, 1024–1029.

Abzhanov A, Tzahor E, Lassar AB, et al. (2003) Dissimilar regulation of cell differentiation in mesencephalic (cranial) and sacral (trunk) neural crest cells *in vitro*. *Development* **130**, 4567–4579.

Bronner-Fraser M (1986) Analysis of the early stages of trunk neural crest migration in avian embryos using monoclonal antibody HNK-1. *Dev Biol* **115**, 44–55.

Burke AC (1989) Development of the turtle carapace: implications for the evolution of a novel bauplan. *J Morphol* **199**, 363–378.

Burke AC (1991) The development and evolution of the turtle body plan. Inferring intrinsic aspects of the evolutionary

process from experimental embryology. *Am Zool* **31**, 616–627.

Burke AC (2009) Turtles again. *Evol Dev* **11**, 622–624.

Carroll RL (2012) Problems of the ancestry of turtles. In: *Morphology and Evolution of Turtles: Origin and Early Diversification* (eds Brinkman DB, Holroyd PA, Gardner JD), pp. 19–36. Dordrecht: Springer.

Cebra-Thomas J, Tan F, Sistla S, et al. (2005) How the turtle forms its shell: a paracrine hypothesis of carapace formation. *J Exp Zool* **304B**, 558–569.

Cebra-Thomas JA, Betters E, Yin M, et al. (2007) Evidence that a late-emerging population of trunk neural crest cells forms the plastron bones in the turtle *Trachemys scripta*. *Evol Dev* **9**, 267–277.

Cebra-Thomas JA, Terrell A, Branyan K, et al. (2013) Late-emigrating trunk neural crest cells in turtle embryos generate an osteogenic ectomesenchyme in the plastron. *Dev Dyn* **242**, 1223–1235.

Claessens LPAM (2004) Dinosaur gastralia; origin, morphology, and function. *J Vertebr Paleontol* **24**, 89–106.

Clark K, Bender G, Murray BP, et al. (2001) Evidence for the neural crest origin of turtle plastron bones. *Genesis* **31**, 111–117.

Crossley PH, Minowada G, MacArthur CA, et al. (1996) Roles for FGF8 in the induction, initiation, and maintenance of chick limb development. *Cell* **84**, 127–136.

Domowicz MS, Mueller MM, Novak TE, et al. (2003) Developmental expression of the HNK-1 carbohydrate epitope on aggrecan during chondrogenesis. *Dev Dyn* **226**, 42–50.

Gaffney ES (1990) The comparative osteology of the Triassic turtle Proganochelys . *Bull Am Mus Nat Hist* **194**, 1–263.

Gegenbaur C (1898) *Vergleichende Anatomie der Wirbelthiere*. Leipzig: Verlag von Wilhelm Engelmann.

Gilbert SF, Loredo GA, Brukman A, et al. (2001) Morphogenesis of the turtle shell: the development of a novel structure in tetrapod evolution. *Evol Dev* **3**, 47–58.

Gilbert SF, Bender G, Betters E, et al. (2007) The contribution of neural crest cells to the nuchal bone and plastron of the turtle shell. *Integr Comp Biol* **47**, 401–408.

Gilbert SF, Cebra-Thomas JA, Burke AC (2008) How the turtle gets its shell. In: *Biology of Turtles* (eds Wyneken J, Godfrey MH, Bels V), pp. 1–16. Boca Raton: CRC Press.

Goodrich ES (1930) *Studies on the Structure and Development of Vertebrates*. London: Macmillan.

Greenbaum E (2002) A standardized series of embryonic stages for the emydid turtle *Trachemys scripta*. *Can J Zool* **80**, 1350–1370.

Gross JB, Hanken J (2008) Review of fate-mapping studies of osteogenic cranial neural crest in vertebrates. *Dev Biol* **317**, 389–400.

Hall BK (1998) *Evolutionary Developmental Biology*. 2nd edn. London: Chapman & Hall.

Hamburger V, Hamilton HL (1951) A series of normal stages in the development of the chick embryo. *J Morphol* **88**, 49–91.

Kawashima-Ohya Y, Narita Y, Nagashima H, et al. (2011) Hepatocyte growth factor is crucial for development of the carapace in turtles. *Evol Dev* **13**, 260–268.

Kuraku S, Usuda R, Kuratani S (2005) Comprehensive survey of carapacial ridge-specific genes in turtle implies co-option of some regulatory genes in carapace evolution. *Evol Dev* **7**, 3–17.

Kuratani S, Nagashima H (2012) A developmental basis for innovative evolution of the turtle shell. In: *From Clone to Bone: The Synergy of Morphological and Molecular Tools in Palaeobiology* (eds Asher RJ, Müller J), pp. 279–300. Cambridge: Cambridge University Press.

Kuratani S, Kuraku S, Nagashima H (2011) Evolutionary developmental perspective for the origin of the turtles: the folding theory for the shell based on the developmental nature of the carapacial ridge. *Evol Dev* **13**, 1–14.

Le Douarin NM (1982) *The Neural Crest*. Cambridge: Cambridge University Press.

Le Douarin NM, Teillet M, Le Lievre C (1977) Influence of the tissue environment on the differentiation of neural crest cells. In: *Cell and Tissue Interaction* (eds Lash JW, Burger MM), pp. 11–27. New York: Raven Press.

Lee RT, Knapik EW, Thiery JP, et al. (2013a) An exclusively mesodermal origin of fin mesenchyme demonstrates that zebrafish trunk neural crest does not generate ectomesenchyme. *Development* **140**, 2923–2932.

Lee RT, Thiery JP, Carney TJ (2013b) Dermal fin rays and scales derive from mesoderm, not neural crest. *Curr Biol* **23**, R336–R337.

Li C, Wu XC, Rieppel O, et al. (2008) An ancestral turtle from the Late Triassic of southwestern China. *Nature* **456**, 497–501.

Loredo GA, Brukman A, Harris MP, et al. (2001) Development of an evolutionarily novel structure: fibroblast growth factor expression in the carapacial ridge of turtle embryos. *J Exp Zool* **291B**, 274–281.

Lubick N (2013) Biologists tell dueling stories of how turtles get their shells. *Science* **341**, 329.

Luider TM, Peters-van der Sanden MJ, Molenaar JC, et al. (1992) Characterization of HNK-1 antigens during the formation of the avian enteric nervous system. *Development* **115**, 561–572.

Luider TM, Bravenboer N, Meijers C, et al. (1993) The distribution and characterization of HNK-1 antigens in the developing avian heart. *Anat Embryol* **188**, 307–316.

Matsuoka T, Ahlberg PE, Kessaris N, et al. (2005) Neural crest origins of the neck and shoulder. *Nature* **436**, 347–355.

McGonnell IM, Graham A (2002) Trunk neural crest has skeletogenic potential. *Curr Biol* **30**, 767–771.

Moignard V, Woodhouse S, Fisher J, et al. (2013) Transcriptional hierarchies regulating early blood cell development. *Blood Cells Mol Dis* **51**, 239–247.

Mongera A, Nüsslein-Volhard C (2013) Scales of fish arise from mesoderm. *Curr Biol* **23**, R338–R339.

Moss ML (1969) Comparative histology of dermal sclerifications in reptiles. *Acta Anat* **73**, 510–533.

Nagase T, Shimoda Y, Sanai Y, et al. (2000) Differential expression of two glucuronyltransferases synthesizing HNK-1 carbohydrate epitope in the sublineages of the rat myogenic progenitors. *Mech Dev* **98**, 145–149.

Nagashima H, Uchida K, Yamamoto K, et al. (2005) Turtle-chicken chimera: an experimental approach to understanding evolutionary innovation in the turtle. *Dev Dyn* **232**, 149–161.

Nagashima H, Kuraku S, Uchida K, et al. (2007) On the carapacial ridge in turtle embryos: its developmental origin, function, and the chelonian body plan. *Development* **134**, 2219–2226.

Nagashima H, Sugahara F, Takechi M, et al. (2009) Evolution of the turtle body plan by the folding and creation of new muscle connections. *Science* **325**, 193–196.

Nagashima H, Kuraku S, Uchida K, et al. (2012a) Body plan of turtles: an anatomical, developmental and evolutionary perspective. *Anat Sci Int* **87**, 1–13.

Nagashima H, Kuraku S, Uchida K, et al. (2012b) Origin of the turtle body plan – The folding theory to illustrate turtle-specific developmental repatterning. In: *Morphology and Evolution of Turtles: Origin and Early Diversification* (eds Brinkman DB, Holroyd PA, Gardner JD), pp. 37–50. Dordrecht: Springer.

Nakamura H, Ayer-le Lievre CS (1982) Mesectodermal capabilities of the trunk neural crest of birds. *J Embryol Exp Morphol* **70**, 1–18.

Ogushi K (1911) Anatomische Studien an der Japanischen dreikralligen Lippenschildkröte (Trionyx japonicus). *Morph Jahrb* **43**, 1–106.

Ohuchi H, Nakagawa T, Yamamoto A, et al. (1997) The mesenchymal factor, FGF10, initiates and maintains the outgrowth of the chick limb bud through interaction with FGF8, an apical ectodermal factor. *Development* **124**, 2235–2244.

Parker WK (1868) *A Monograph on the Structure and Development of the Shoulder-Girdle and Sternum in the Vertebrates*. London: Ray Society.

Pennisi E (2004) Neural beginnings for the turtle's shell. *Science* **303**, 951.

Rieppel O (2001) Turtles as hopeful monsters. *BioEssays* **23**, 987–991.

Romer AS (1956) *Osteology of Reptiles*. Chicago: University of Chicago Press.

Ruckes H (1929) Studies in chelonian osteology part II, The morphological relationships between the girdles, ribs and carapace. *Ann N Y Acad Sci* **31**, 81–120.

Sánchez-Guardado LO, Puelles L, Hidalgo-Sanchez M (2013) *Fgf10* expression patterns in the developing chick inner ear. *J Comp Neurol* **521**, 1136–1164.

Serra JA (1946) Histochemical tests for protein and amino acids: the characterization of basic proteins. *Stain Technol* **21**, 5–18.

Shimada A, Kawanishi T, Kaneko T, et al. (2013) Trunk exoskeleton in teleosts is mesodermal in origin. *Nat Commun* **4**, 1639. doi:10.1038/ncomms2643.

Shimomura Y, Agalliu D, Vonica A, et al. (2010) APCDD1 is a novel Wnt inhibitor mutated in hereditary hypotrichosis simplex. *Nature* **464**, 1043–1047.

Smith MM, Hall BK (1990) Developmental and evolutionary origins of vertebrate skeletogenic and odontogenic tissues. *Biol Rev* **65**, 277–374.

Tabin C, Wolpert L (2007) Rethinking the proximodistal axis of the vertebrate limb in the molecular era. *Gen Dev* **21**, 1433–1442.

Takahashi M, Fujita M, Furukawa Y, et al. (2002) Isolation of a novel human gene, *APCDD1*, as a direct target of the β-catenin/T-cell factor 4 complex with probable involvement in colorectal carcinogenesis. *Cancer Res* **62**, 5651–5656.

Tamura K, Kuraishi R, Saito D, et al. (2001) Evolutionary aspects of positioning and identification of vertebrate limbs. *J Anat* **199**, 195–204.

Tanaka M (2013) Molecular and evolutionary basis of limb field specification and limb initiation. *Dev Growth Differ* **55**, 149–163.

Theißen G (2006) The proper place of hopeful monsters in evolutionary biology. *Theory Biosci* **124**, 349–369.

Theißen G (2009) Saltational evolution: hopeful monsters are here to stay. *Theory Biosci* **128**, 43–51.

Tokita M, Kuratani S (2001) Normal embryonic stages of the Chinese softshelled turtle *Pelodiscus sinensis*. *Zool Sci* **18**, 705–715.

True JR, Carroll SB (2002) Gene co-option in physiological and morphological evolution. *Annu Rev Cell Dev Biol* **18**, 53–80.

Vickaryous MK, Sire JY (2009) The integumentary skeleton of tetrapods: origin, evolution, and development. *J Anat* **214**, 441–464.

Wang Z, Pascual-Anaya J, Zadissa A, et al. (2013) The draft genomes of soft-shell turtle and green sea turtle yield insights into the development and evolution of the turtle-specific body plan. *Nat Genet* **45**, 701–706.

Yntema CL (1968) A series of stages in the embryonic development of *Chelydra serpentina*. *J Morphol* **125**, 219–251.

Yu J, Freud AG, Caligiuri MA (2013) Location and cellular stages of natural killer cell development. *Trends Immunol* **34**, 573–582.

Zangerl R (1939) The homology of the shell elements in turtles. *J Morphol* **65**, 383–409.

Zangerl R (1969) The turtle shell. In: *The Biology of the Reptilia*, **Vol. 1**. (eds Gans C, Bellairs Ad'A, Parsons TS), pp 311–319, New York: Academic Press.

Supporting Information

Additional Supporting Information may be found in the online version of this article:

Fig. S1. Expression of *Fgf10* in *Trachemys scripta* embryos.

Fig. S2. Expression of the HNK-1 epitope in the humerus of *Gallus gallus*.

Video S1. Three-dimensional reconstruction of the stage 17 *Trachemys scripta* embryo shown in Fig. 4.